Effects of Nd : YAG laser surface treatment on tribological properties of cold-sprayed Ti-6Al-4V coatings tested against 100Cr6 steel under dry condition

Khun, Nay Win; Tan, Adrian Wei Yi; Sun, Wen; Liu, Erjia

2019

Khun, N. W., Tan, A. W. Y., Sun, W., & Liu, E. (2019). Effects of Nd : YAG laser surface treatment on tribological properties of cold-sprayed Ti-6Al-4V coatings tested against 100Cr6 steel under dry condition. Tribology Transactions, 62(3), 391-402. doi:10.1080/10402004.2018.1563258

https://hdl.handle.net/10356/145291

https://doi.org/10.1080/10402004.2018.1563258

Effects of Nd:YAG laser surface treatment on tribological properties of cold sprayed Ti-6Al-4V coatings tested against 100Cr6 steel under dry condition

N. W. Khun, A. W. Y. Tan, W. Sun, E. Liu*

Rolls-Royce@NTU Corporate Lab, Nanyang Technological University, 50 Nanyang Avenue, Singapore 639798, Singapore

School of Mechanical and Aerospace Engineering, Nanyang Technological University

50 Nanyang Avenue, Singapore 639798, Singapore

*Corresponding author: MEJLiu@ntu.edu.sg, Tel: +65-67905504

ABSTRACT

The surfaces of cold sprayed Ti-6Al-4V (Ti64) coatings were laser irradiated with different laser powers of 50-200 W to study the effects of Nd:YAG laser surface treatment on their tribological properties. The hardness of the laser treated Ti64 coatings became higher with higher laser power due to the more rapid cooling caused by a larger temperature difference between the coating temperature and room temperature. The wear of the laser treated Ti64 coatings tested against 6 mm 100Cr6 steel balls under dry condition at room temperature decreased with increased laser power as a result of their increased surface wear resistance associated with their increased surface hardness. It could be concluded that the laser surface treatment of the cold sprayed Ti64 coatings improved their surface wear resistance compared to that of the untreated Ti64 coatings.

KEYWORDS: Cold spray; laser surface melting; laser power; Ti-6Al-4V; hardness; wear

INTRODUCTION

Thermal spray processes are widely used in aerospace industry for repair purposes due to their versatilities and high deposition rates, and a wide range of applicable materials [1]. However, metallic coatings produced via thermal spray processes have high porosity and oxidation levels, high thermal residual stress, and so on [2-8]. Therefore, low temperature cold spray process is considered as an alternative process to produce metallic coatings with much lower porosity and oxidation levels, lack of thermal residual stress, cold worked microstructure, and higher thickness compared to those of thermally sprayed metallic coatings [2-8]. Unfortunately, the private nature of the cold spray technology and its research and development stage make available data on the tribological properties of cold sprayed metallic coatings insufficient for successful applications [5].

Ti-6Al-4V (Ti64) alloy is widely used for aerospace applications because it possesses high specific strength, high elastic modulus, light weight, and high corrosion resistance [5-11]. However, the poor abrasive wear resistance of Ti64 alloy limits its tribology related applications. Several researchers reported that cold sprayed metallic coatings had higher wear resistance than their relevant commercial metals [5, 6, 12-14]. It is therefore expected that cold spraying of Ti64 particles could produce high wear resistant Ti64 coatings for aerospace applications. Besides, surface modification of repaired Ti64 aerosapce components using cold spray technology should be further considered to promote their service life and performance via their improved surface wear resistance.

Laser surface engineering can be considered as a potential approach to modify the surfaces of different solid materials because the capability of high energy laser beams to generate rapid rates of heating and cooling can give rise to changes in their surface properties such as grain refinement, morphological change, phase transformation, and compositional change via a non-equilibrium cooling without changing the bulk properties [15-20]. In addition, laser surface melting is a direct process to provide uniform surface structure. Therefore, laser surface melting does not have any issue regarding poor adhesion of laser treated surface with bulk material in contrast to coating methods [15-20]. Moreover, laser surface melting has been proved as a promising surface treatment to improve the surface properties of materials such as mechanical, corrosion, wear, and wettability properties [15-20]. Adel et al [15] reported that Nd:YAG laser treated acicular bainitic ductile iron had higher wear resistance than as-casted iron. Sagaro et al [16] found that the laser surface treatment resulted in the higher wear resistance of U13A steel compared to conventional heat treatments. Singh et al [17] investigated the effects of laser surface treatment on the corrosion and wear resistance of Ti64 alloy and found that laser treated Ti64 alloy had higher corrosion and wear resistance than untreated one. Matsukawa et al [18] discovered that the laser surface treatment of electroless Ni-P plated coatings gave rise to their higher corrosion and wear resistance compared to those of untreated ones. It was reported [19] that laser surface hardened EN25 steel exhibited lower friction and wear at elevated temperatures than untreated one. The results clearly show that the laser surface treatment improves the surface wear resistance of metallic materials. However, the data on the tribological properties of laser treated Ti64 alloys, especially cold sprayed Ti64 coatings, are not available for successful tribological applications. Since the laser power is one of the most important laser treatment parameters affecting the surface properties of Ti64 alloys, an understanding of the effects of laser power on the tribological properties of laser treated Ti64 alloys is important to successfully apply the laser surface treatment process in aerospace repair applications.

In this study, cold sprayed Ti64 coatings were deposited on commercial Ti64 substrates via a high pressure cold spray process. Then, the surfaces of the cold sprayed Ti64 coatings were laser irradiated with different laser powers of 50-200 W. The surface topographies and morphologies of the laser treated Ti64 coatings were studied using surface profilometry (SP) and scanning electron microscopy (SEM), respectively. The hardness of the laser treated Ti64 coatings was measured with Vickers micro-hardness test. The friction and wear of the laser treated Ti64 coatings tested against 100Cr6 steel balls under dry condition at room temperature (RT ~ 22-24 °C) were measured using ball-on-disk micro-tribological test that conformed to DIN50324 and ASTM G99.

EXPERIMENTAL DETAILS

SAMPLE PREPARATION

Ti64 coatings were cold sprayed on commercial Ti64 substrates (Grade 5) with 50 mm × 50 mm × 8 mm using a high pressure cold spray system with commercial Ti64 powder (size: 1-45 μm). The optimized cold spray process parameters were gas temperature of 950 °C, gas pressure of 2.5 MPa, nozzle/scan speed of 100-400 mm/s, spray angle of 90°, and stand-off distance of 25 mm. The helium (He) working gas was used during the cold spraying. The cold sprayed Ti64 coatings with a thickness of about 3000 μm were wire cut to get square pieces with 10 mm × 10 mm followed by polishing with 1200 grit papers at the final stage, cleaning with an ethanol in an ultrasonic bath for 20 min, and air drying prior to the laser surface treatment.

The laser surface irradiation of the cold sprayed Ti64 coatings was carried out by using a 500 watt (W) nanosecond pulsed Nd:YAG laser with a wavelength of 1064 nm, a frequency of 12000 Hz, and a pulse duration of 38 ns. The laser treatment parameters optimized in this study were laser powers 10% (50 W), 20% (100 W), 30% (150 W), and 40% (200 W) of a total laser power, a repetition rate of 10000 Hz, a scanning speed of 20 mm/s, a 70% overlap, and a pulse width of 10 μs. The flat top hat beam (focal length of 152.5 mm) was defocused up to 1 mm. The side length of the laser beam was about 0.6 mm. The laser surface treatment was conducted in a closed chamber with a vacuum machine provided to remove dust. The laser treated surfaces were cleaned with an ethanol in an ultrasonic bath for 30 min prior to the following characterization.

CHARACTERIZATION

The surface and cross-sectional microstructures of the cold sprayed Ti64 coating were observed using an optical microscopy (OM). The detailed sample preparation procedure for the microstructural evaluation was described elsewhere [5, 7, 8].

The cross-sectional porosity level of the cold sprayed Ti64 coating was obtained by analyzing its OM micrographs (before etching) captured with 5× lens using ImageJ software, and averaged from its six OM micrographs [5, 7, 8].

The surface topographies and morphologies of the laser treated Ti64 coatings were measured using SP with a diamond stylus of 4 µm in diameter and SEM [5], respectively. Three measurements per coating in a scan size of 1 mm × 1 mm were conducted to get an average root-mean-squared surface roughness, R_q.

The hardnesses of the laser treated Ti64 coatings were measured using Vickers micro-hardness test under a normal load of 200 g (1.96 N) [5]. Twelve measurements randomly carried out on each surface were calculated to get an average hardness.

The wear morphologies of the 100Cr6 steel balls were observed using OM [5].

A ball-on-disk micro-tribological test was applied to evaluate the tribological properties of the laser treated Ti64 coatings at RT [5]. A 100Cr6 steel ball of 6 mm in diameter was rotated on the laser treated Ti64 coating surface in a circular path of 1 mm in radius for 30000 laps (total sliding distance of 188 m) at a sliding speed of 3 cm/s under a normal load of 1 N at RT (55-60 % relative humidity). Three measurements per coating were carried out to get average tribological results. The specific wear rates were calculated from the widths and depths of wear tracks measured using SP. The estimated maxium Hertzian contact pressure for the (6 mm 100Cr6 steel ball) sphere-on-flat plate (cold sprayed Ti64 coating) configuration under a normal load of 1 N was 460 MPa.

RESULTS AND DISCUSSION

Fig. 1a shows the surface microstructure of the cold sprayed Ti64 coating on which individual particles and their interfaces can be clearly seen. Fig. 1b shows the cross-sectional microstructure of the same coating on which flattened Ti64 particles are found as a result of their severe deformaiton during the cold spraying [5, 7]. The cross-sectional porosity level of the cold sprayed Ti64 coating measured before etching is 2.53±0.4%. The black spots in the cross-sectional microstructure of the cold sprayed Ti64 coating (Fig. 1b) probably result from preferential etching of particle interfaces during etching of the coating for the microstructural evaluation.

Figs. 2a and b show the surface topography and morphology of the polished/untreated Ti64 coating, respectively, on which a smooth surface is found.

Fig. 3 shows the surface topographies and morphologies of the laser treated Ti64 coatings with different laser powers. As the surfaces of the laser treated Ti64 coatings become rougher with higher laser power as found in Figs. 3a-d, the laser treated Ti64 coating with the highest laser power of 200 W has the highest surface roughness (Fig. 3d) because the most rapid cooling caused by the largest temperature difference between the coating temperature and RT results in protruded asperities and dimples on the surface topography via the most severe surface shrinkage [20-22]. As shown by the comparison of Figs. 3a and b, the laser treated Ti64 coating with higher laser power has a more apparently cracked surface. In Fig. 3c, fish-bone-shaped-cracks are found along the laser irradiated lines on the surface of the laser treated Ti64 coating with 150 W. When the Ti64 coating is laser irradiated with 200 W, the severe surface shrinkage forms more apparent cracks on its surface as shown in Fig. 3d [20-22]. The surface observation shows that the laser treated Ti64 surface becomes more brittle and more cracked with higher laser power via the more rapid cooling of the surface.

Fig. 4 presents the R_q values of the untreated Ti64 coating and laser treated Ti64 coatings with different laser powers. The R_q value of the polished/untreated Ti64 coating is about 0.26 μm. The laser treated Ti64 coating with a laser power of 50 W has a larger R_q value of about 0.3 μm than the untreated Ti64 coating while increasing the laser power to 150 W increases the R_q value of the laser treated Ti64 coating to about 0.45 μm. The laser treated Ti64 coating with the highest laser power of 200 W has the largest R_q value of about 2.3 μm due to the most apparently protruded asperities above its surface and formed dimples on its surface (Fig. 3d) [20-22]. It can be deduced that the laser surface treatment apparently roughens the surfaces of the cold sprayed Ti64 coatings.

Fig. 5 illustrates the XRD patterns of the untreated Ti64 coating and laser treated Ti64 coatings with different laser powers. The XRD patterns of the laser treated Ti64 coatings are apparently different from that of the untreated Ti64 coating as a result of the formation of hard α″ martensitic phases in their surface microstructures associated with the rapid cooling of their laser treated surfaces [23, 24]. It clearly indicates that the laser surface treatment of the cold sprayed Ti64 coatings gives rise to significant changes in their surface microstructures associated with the formation of hard α″ martensitic phases [23, 24].

Fig. 6 shows the hardnesses of the untreated Ti64 coating and laser treated Ti64 coatings with different laser powers. The hardness of the untreated Ti64 coating is about 414 Hv (4.06 GPa). The laser treated Ti64 coating with a laser power of 50 W has higher hardness of 426 Hv (4.19 GPa) than the untreated Ti64 coating. Increasing the laser power to 150 W increases the hardness of the laser treated Ti64 coatings to about 464 Hv (4.55 GPa). The laser surface treatment of the Ti64 coating with a laser power of 200 W dramatically increases its hardness to 705 Hv (6.91 GPa). It is clear that the laser surface treatment enhances the surface hardness of the Ti64 coatings via the formation of hard α″ martensitic phases in their surface microstructures associated with the rapid cooling of their laser treated surfaces [23]. The higher laser power therefore gives rise to the higher surface hardness of the laser treated Ti64 coatings as a result of the more rapid cooling caused by the larger temperature difference between the coating temperature and RT. Since the laser surface treatment with a larger effective depth could result in the formation of a thicker laser treated surface layer, it is hypothesized that the thicker and harder laser treated surface layers of the laser treated Ti64 coatings with higher laser powers are responsible for their higher surface hardnesses.

Fig. 7 presents the friction coefficients of the untreated Ti64 coating and laser treated Ti64 coatings with different laser powers tested against 100Cr6 steel balls . The friction coefficient of the untreated Ti64 coating is about 0.52. The laser treated Ti64 coating with a laser power of 50 W has a higher friction coefficient of about 0.59 than the untreated Ti64 coating. It was reported that an effective interfacial shear strength between two contacting surfaces gave rise to high friction [5, 6, 25-31]. The wear of rubbing surfaces resulted in surface roughening and production of wear debris, which in turn lowered the friction by reducing the interfacial shear strength between them [32-35]. Therefore, it is supposed that the improved wear resistance of the laser treated Ti64 coating with 50 W is responsible for its higher friction via less roughening of rubbing surfaces and smaller amount of wear debris produced. As a result, the increased laser power to 150 W increases the friction coefficient of the laser treated Ti64 coatings to about 0.66 by further lessening roughening of rubbing surfaces and decreasing production of wear debris. However, the friction coefficient of the laser treated Ti64 coating with 200 W turns to decrease to about 0.57. The possible reason is that the protruded/hard asperities in a line pattern (Fig. 3d) above the surface apparently reduce a contact area between the steel ball and coating for the decreased friction of the coating [25-31].

The effect of surface roughness on the friction of the laser treated Ti64 coatings should be taken into account because a rougher surface can give rise to higher friction via mechanical interlocking between asperities of two rubbing surfaces [5, 6, 11, 34]. Therefore, the increased friction of the laser treated Ti64 coatings with increased laser power from 0 to 150 W (Fig. 7) can be correlated to their increased surface roughness (Fig. 4). Although the highest surface roughness of the laser treated Ti64 coating with the highest laser power of 200 W should result in its highest friction, its lowered friction compared to those of the other laser treated Ti64 coatings implies that the apparently protruded asperities in a line pattern above the surface (Fig. 3d) reduce a contact area between the steel ball and laser treated Ti64 coating for decreasing the friction [25-31].

Fig. 8 shows the friction coefficients of the uncoated Ti64 coating and laser treated Ti64 coatings with different laser powers as a function of the number of laps. The untreated Ti64 coating exhibits stable friction throughout the wear test as a result of its stable wear [5, 6, 11, 29-31, 34]. The laser treated Ti64 coatings with laser powers of 50, 100, and 150 W exhibit similar friction coefficients for about 10000 laps and higher stable friction coefficients for the rest, especially for the higher laser powers. The laser treated Ti64 coating with a laser power of 200 W has the lower trend of friction coefficient versus laps than the other laser treated Ti64 coatings. The untreated Ti64 coating has a larger fluctuation in its friction coefficient with respect to the number of laps than the laser treated Ti64 coatings probably due to the more significant stick-slip phenomena occurred during the sliding [36].

Fig. 9 shows the wear topographies of the untreated Ti64 coating and laser treated Ti64 coatings with different laser powers tested against 100Cr6 steel balls. The untreated Ti64 coating has a significant wear track on its surface with a specific wear rate of 93.9 ± 5.8 × 10^{-14} m^3/(Nm) as found in Fig. 9a. The specific wear rate of the laser treated Ti64 coating with 50 W is 88.2 ± 2.2 × 10^{-14} m^3/(Nm), implying that the laser treated Ti64 coating with 50 W (Fig. 9b) has lower wear than the untreated Ti64 coating (Fig. 9a) [29, 37, 38]. In Figs. 9c-e, the laser treated Ti64 coatings with laser powers of 100-200 W do not show measurable wear tracks on their surfaces. It is clear that the laser surface treatment of the cold sprayed Ti64 coatings with the laser powers of 100-200 W effectively prevents their surface wear during prolonged rubbing contact with the counter steel balls.

Fig. 10 presents SEM images showing the wear morphologies of the untreated Ti64 coating and laser treated Ti64 coatings with different laser powers tested against 100Cr6 steel balls. Although the wear tracks on the wear topographies of the laser treated Ti64 coatings with laser powers of 100-150 W (Figs. 9b-e) are not measureable, their wear morphologies can be clearly seen in their SEM images (Figs. 10b-e). Comparison of Figs. 10a and 10b shows that the laser treated Ti64 coating with 50 W has a smaller wear width than the untreated Ti64 coating, which indicates that the laser surface treatment with 50 W improves the surface wear resistance of the cold sprayed Ti64 coating. The laser surface treatment of the Ti64 coating with the higher laser power of 100 W further improves its surface wear resistance so that its wear width (Fig. 10c) is apparently smaller than that of the laser treated one with 50 W (Fig. 10a). Furthermore, the increased laser power to 150 W results in the further decreased wear width of the laser treated Ti64 coating via its increased surface wear resistance as shown in Fig. 10d. As shown by the comparison of Figs. 10c and 10d, thicker tribolayers are found on the wear track of the laser treated Ti64 coating with the higher laser power of 150 W because the higher surface wear resistance of the laser treated Ti64 coating allows more compaction of wear debris to form the thicker tribolayers [5, 6, 11, 39, 40]. In addition, a detachment of the tribolayers is found on the wear track of the laser treated Ti64 coating with 150 W. In Figs. 10b, c, and d, the laser treated Ti64 coatings with the laser powers more than 50 W have much smoother wear morphologies with much smaller amount of wear debris. The wear morphology of the laser treated Ti64 coating with 200 W (Fig. 10e) is different from those of the other laser treated Ti64 coatings (Figs. 10b, c and d) because the highest surface wear resistance of the laser treated Ti64 coating with 200 W allows only the wearing of protruded asperities above its surface during the sliding. However, the wider wear width of the laser treated Ti64 coating with 200 W (Fig. 10e) compared to that of the laser treated Ti64 coating with 150 W (Fig. 10d) indicates that the higher surface roughness causes a larger interaction between the steel ball and coating via higher vibration of the sliding system [26, 29]. It can be deduced that the laser surface treatment with the laser powers more than 50 W results in a significant improvement in the surface wear resistance of the cold sprayed Ti64 coatings via their enhanced surface hardness.

Fig. 11a shows the energy dispersive X-ray (EDX) spectrum of the untreated Ti64 coating on which C, O, Ti, Al and V peaks are mainly detected. The C peak results from the surface carbon contaminant [41, 42]. The Ti, Al and V peaks come from the Ti64 matrix. In Figs. 11b, c, d, and e, the laser treated Ti64 coatings with different laser powers have similar EDX spectra to that of the untreated Ti64 coating (Fig. 11a). However, the O peaks on the EDX spectra of the laser treated Ti64 coatings become stronger with higher laser powers, indicating the increased surface oxidation of the laser treated Ti64 coatings [43-46].

Figs. 11f-11j show the EDX spectra measured on the wear tracks of the untreated Ti64 coating and laser treated Ti64 coatings with different laser powers tested against 100Cr6 steel balls on which C, O, Ti, Al and V peaks are commonly found. The O peaks measured on the wear tracks of the untreated Ti64 coating (Fig. 11f) and laser treated Ti64 coating with a laser power of 50 W (Fig. 11g) are not stronger than those measured on their untested areas (Figs. 11a and 11b). However, the O peaks measured on the wear tracks of the laser treated Ti64 coatings with laser powers of 100-

200 W (Figs. 11h, i, and j) are apparently stronger than those measured on their untested areas (Figs. 11c, d, and e) as well as those measured on the wear tracks of the untreated Ti64 coating and laser treated Ti64 coating with 50 W (Figs. 11a and b). It indicates that the higher surface wear resistance of the laser treated Ti64 coatings with laser powers of 100-200 W than that of the untreated Ti64 coating and laser treated Ti64 coating with 50 W results in higher frictional heating, which in turn gives rise to their more severe surface oxidation during the prolonged sliding [5, 6, 47, 48]. In addition, the depressed Ti and Al peaks on the EDX spectra measured on the wear tracks of the laser treated Ti64 coatings with 100-200 W (Figs. 11h, i, and j) indicate that their wear tracks are significantly covered by the oxidized layers. Furthermore, additional Fe peaks on the EDX spectra of their wear tracks (Figs. 11h, i, and j) imply that their improved surface wear resistance results in the significant wear of their counter steel balls.

Figs. 12a and b show the wear morphologies of the steel balls slid on the untreated Ti64 coating and laser treated Ti64 coating with a laser power of 200 W, respectively. The steel balls slid on the untreated Ti64 coating and laser treated Ti64 coating with 50 W exhibit elongated wear scars on their surfaces while circular shaped wear scars are found on the surfaces of the steel balls rotated on the laser treated Ti64 coatings with 100-200 W. The reason is that the lower surface wear resistance of the untreated Ti64 coating and laser treated Ti64 coating with 50 W compared to that of the laser treated Ti64 coatings with 100-200 W gives rise to a larger interaction between the steel balls and coatings via the higher wear of the coatings. The improved surface wear resistance of the laser treated Ti64 coatings with 100-200 W results in the preferential wear and subsequently the circular shaped wear scars of their counter steel balls. As shown by the comparison of Figs. 12a and b, larger ploughed furrows are found on the worn surface of the steel ball slid on the laser treated Ti64 coating with 200 W (Fig. 12b) because the higher surface roughness of the laser treated Ti64 coating compared to that of the untreated Ti64 coating serves as an abrading surface to result in the more severe abrasive wear of its counter steel ball [34].

CONCLUSIONS

In this study, the surfaces of the cold sprayed Ti64 coatings were irradiated using Nd:YAG laser with different laser powers of 50-200 W. The tribological properties of the laser treated Ti64 coatings tested against 100Cr6 steel balls were systematically investigated with respect to the laser power. The following conclusions were drawn.

- The surface roughness of the laser treated Ti64 coatings became higher with higher laser power so that the laser treated Ti64 coating with the highest laser power of 200 W had the highest surface roughness attributed to dimples and protruded asperities on its surface.
- The laser treated Ti64 coating with the higher laser power had higher surface hardness as a result of the more rapid cooling caused by a larger temperature difference between the coating temperature and RT.
- The wear of the laser treated Ti64 coating with 50 W was apparently lower than that of the untreated Ti64 coating as a result of the improved surface wear resistance of the laser treated Ti64 coating associated with its enhanced surface hardness. As the increased laser power increased the surface wear resistance of the laser treated Ti64 coatings via their increased surface hardness, the laser treated Ti64 coatings with 100-200 W did not show measurable wear tracks on their surfaces.
- The results clearly showed that the tribological properties of the laser treated Ti64 coatings were significantly influenced by the laser power.

ACKNOWLEDGEMENTS

Authors are grateful for the financial support from the National Research Foundation (NRF), Rolls-Royce (RR), and Nanyang Technological University (NTU), Singapore, with the NRF-RR-NTU research grant number of M-RT3.1, and the project team members from RR, Singapore, Anna Tai and Nicholas Weeks for their contributions to this work. W. Sun is grateful to NTU for his PhD scholarship.

REFERENCES

[1] Cizek, J. and Khor, K. A. (2012), Role of in-flight temperature and velocity of powder particles on plasma sprayed hydroxyapatite coating characteristics, Surf. Coat. technol. 206(8-9) pp. 2181-2191.

[2] Singh, H., Sidhu, T. S. and Kalsi, S. B. S. (2012), Cold spray technology: Future of coating deposition processes, Frattura ed Integrita Strutturale 22, pp. 69-84.

[3] Klinkov, S. V., Kosarev, V. F. and Rein, M. (2005), Cold spray deposition: Significant of particle impact phenomena, Aerospace Sci. Technol. 9, pp. 582-591.

[4] Assadi, H., Schmidt, T., Richter, H., Kliemann, J. O., Binder, K., Gartner, F., Klassen, T. and Kreye, H. (2011), On parameter selection in cold spraying, J. Thermal Spray Technol. 20(6), pp. 1161-1176.

[5] Khun, N. W., Tan, A. W. Y. and Liu, E. (2016), Mechanical and tribological properties of cold sprayed Ti coatings on Ti-6Al-4V substrates, J. Thermal Spray Technol. 25(4), pp. 715-724.

[6] Khun, N. W., Li, R. T., Loke, K. and Khor, K. A. (2015), Effects of Al-Cr-Fe quasicrystal content on tribological properties of cold sprayed titanium composite coatings, Tribo. Transa. 58(4), pp. 616-624.

[7] Khun, N. W., Tan, A. W. Y. and Liu, E. (2016), Effect of working pressure on wear and corrosion resistance of cold sprayed Ti-6Al-4V coatings, Surf. Coat. Technol. 302, pp. 1-12.

[8] Khun, N. W., Tan, A. W. Y., Sun, W. and Liu, E. (2017), Effect of heat treatment temperature on microstructure, and mechanical and tribological properties of cold sprayed Ti-6Al-4V coatings, Tribo. Transa. 60(6), pp.1033-1042.

[9] Leyens, C. and Gedanitz, H. (1999), Long-term oxidation of orthorhombic alloy Ti-22Al-25Nb in air between 650 and 800 °C, Scripta Mater. 41(8), pp. 901−906.

[10] Ralison, A., Dettemwamger, G. and Schutze, M. (2000), Oxidation of orthorhombic Ti2AlNb alloys at 800 ℃ in air, Mater. Corros. 51(5), pp. 317–328.

[11] Khun, N. W., Li, R. T. and Khor, K. A. (2015), Mechanical and tribological properties of spark plasma sintered titanium composites filled with different Al-Cr-Fe quasicrystal content, Tribo. Transa. 58(5), pp. 859-866.

[12] Pitchuka, S. B., Boesl, B., Zhang, C., Lahiri, D., Nieto, A., Sundararajan, G. and Agarwal, A. (2014), Dry sliding wear behavior of cold sprayed aluminum amorphous/nanocrystalline alloy coatings, Surf. Coat. Technol. 238, pp. 118-125.

[13] Bakshi, S. R., Wang, D., Price, T., Zhang, D., Keshri, A. K. K., Chen, Y., McCartney, D. G. and Shipway, P. H. (2009), A. Agarwal, Microstructure and wear properties of aluminium/aluminium-silicon composite coatings prepared by cold spraying, Surf. Coat. Technol. 204, pp. 503-510.

[14] Hussain, T., McCartney, D. G., Shipway, P. H. and Marrocco, T. (2011), Corrosion behaviour of cold sprayed titanium coatings and free standing deposits, J. Thermal Spray Technol. 20(1), pp. 260-274.

[15] Adel, K. M., Dhia, A. S. and Ghazali, M. J. (2009), The effect of laser surface hardening on the wear and friction characteristics of acicular bainitic ductile iron, Int. J. Mech. Mater. Eng. 4(2), pp. 167-171.

[16] Sagaro, R., Ceballos, J. S., Blanco, A. and Mascarell, J. (1999), Tribological behaviour of line hardening of steel U13A with Nd:YAG laser, Wear 225-229, pp. 575-580.

[17] Singh, R., Kurella, A. and Dahotre, N. B. (2006), Laser surface modification of Ti-6Al-4V: Wear and corrosion characterization in simulated biofluid, J. Biomater. Appl. 21(1), pp. 49-73.

[18] Matsukawa, K., Kataoka, M. and Morinushi, K. (1994), The effect of pulsed laser annealing on wear and corrosion properties of electroless Ni-P plating, Tribo. Transa. 37(3), pp. 573-579.

[19] Babu, P. D., Buvanashekaran, G. and Balasubramanian, K. R. (2015), The elevated temperature wear analysis of laser surface hardened EN25 steel using response surface methodology, Tribo. Transa. 58(4), pp. 602-615.

[20] Indira, K., Sylvie, C., Zhongke, W. and Hongyu, Z. (2016), Investigation of wettability properties of laser surface modified rare earth Mg alloy, Procedia Eng. 141, pp. 63-69.

[21] Xue, L., Islam, M., Koul, A. K., Bibby, M. and Wallace, W. (1997), Laser gas nitriding of Ti-6Al-4V Part 2: Characteristics of nitrided layers, Adv. Performance Mater. 4(4), pp. 389-408.

[22] Yibas, B. S., Akhtar, S. S., Matthews, A., Karatas, C. and Leyland, A. (2011), Microstructure and thermal stress distribution in laser carbonnitriding treatment of Ti-6Al-4V alloy, J. Manuf. Sci. Eng. 133, pp. 021013-1-8.

[23] Zheng, L. and T. R. Bieler, T. R. (2005), Effects of working, heat treatment, and aging on microstructural evolution and crystallographic texture of α, α′, α″ and β phases in Ti–6Al–4V wire, Mater. Sci. Eng. A 392(1-2), pp. 403-414.

[24] Guo, S., Meng, Q., Zhao, X., Wei, Q. and Xu. H. (2015), Design and fabrication of a metastable β-type titanium alloy with ultralow elastic modulus and high strength, Sci. Rep. 5 (14688), pp. 1-8.

[25] Kato, K. (2000), Wear in relation to friction - a review, Wear 241, pp. 151-157.

[26] Chowdhury, M. A., Khalil, M. K., Nuruzzaman, D. M. and Rahaman, M. L. (2011), The effect of sliding speed and normal load on friction and wear property of aluminium, Int. J. Mech. Mechatron. Eng. 11(1), pp. 45-49.

[27] Okada, M., Liou, N. S., Prakash, V. and Miyoshi, K. (2001), Tribology of high speed metal on metal sliding at near melt and fully melt interfacial temperatures, Wear 249, pp. 672-686.

[28] Chowdhury, M. A., Nuruzzaman, D. M. and Hannan, M. A. (2012), Effect of sliding velocity and relative humidity on friction coefficient of brass sliding against different steel counterfaces, Int. J. Eng. Res. Appl. 2(2), pp. 1425-1431.

[29] Khun, N. W., Frankel, G. S. and Sumption, M. (2014), Effects of normal load, sliding speed and surface roughness on tribological properties of niobium under dry and wet conditions, Tribo. Transa. 57(5), pp. 944-954.

[30] Khun, N. W., E. Liu, Tan A. W. Y., Senthilkumar, D., Albert, B. and Lal, D. M. (2015), Effect of deep cryogenic treatment on mechanical and tribological properties of AISI D3 tool steel, Friction 3(3), pp. 234-242.

[31] Khun, N. W., Yu, H., Chong, Z. Z., Tian, P., Tian, Y., Tor. S. B. and Liu, E. (2016), Mechanical and tribological properties of Zr based bulk metallic glass for sports application, Mater. Design 92, pp. 667-673.

[32] Qu J., Blau P J, Watkins T. R., Cavin O. B. and Kulkarni N. S. (2005), Friction and wear of titanium alloys sliding against metal, polymer and ceramic counterfaces. Wear 258, pp. 1348-1356.

[33] Bhushan B. (1996), Tribology and Mechanics of Magnetic Storage Device. 2nd edition, Springer-Verleg, New York.

[34] Khun, N. W., Trung, P. Q. and Butler, D. L. (2016), Mechanical and tribological properties of shot peened SAE 1070 steel, Tribo. Transa. 59(5), pp. 932-943.

[35] Khun, N. W., Toh, W. Q., Tan, X. P., Liu, E. and Tor, S. B. (2018), Tribological properties of three-dimensionally printed Ti-6Al-4V material via electron beam melting process tested against 100Cr6 without and with Hank's solution, ASME J. Tribo, 140(6), pp. 061606.

[36] Awrejcewicz, J. and Olejnik, P. (2007), Occurrence of stick-slip phenomenon, J. Theo. App. Mech. 45(1), pp. 33-40.

[37] Wang, J., Yan, F. and Xue, Q. (2009), Tribological behaviour of PTFE sliding against steel in sea water, Wear 267, pp. 1634-1641.

[38] Jahanmir, S., Ozmen, Y. and Ives, L. K. (2004), Water lubrication of silicon nitride in sliding, Tribo. Lett. 17(3), pp. 409-417.

[39] Zhang, Q. Y., Zhou, Y., Wang, L., Cui, X. H. and Wang, S. Q. (2016), Investigation on tribolayers and their function of a titanium alloy during dry sliding, Tribo. Inter. 94, pp. 541-549.

[40] Dalili, N., Edrisy, A., Farokhzadeh, K., Li, J., Lo, J. and Riahi, A. R. (2010), Improving the wear resistance of Ti-6Al-4V /TiC composites through thermal oxidation, Wear 269, pp. 590-601.

[41] Khun, N. W., Liu, E., Yang, G. C., Ma, W. G. and Jiang, S. P. (2009), Structure and corrosion behaviour of platinum/ruthenium/nitrogen doped diamond-like carbon thin films, J. Appl. Phys. 106(1), pp. 013506.

[42] Korotin, D. M., Bartkowski, S., Kurmaev, E. Z., Meumann, M., Yakushina, E. B., Valiev, R. Z. and Cholakh, S. O. (2012), Surface characterization of titanium implants treated in hydrofluoric acid, J. Biomater. Nanobiotech. 3, pp. 87-91.

[43] Biswas, A., Li, L., Maity, T. K., Chatterjee, U. K., Mordike, B. L., I. Manna, I. and Majumdar, J. D. (2007), Laser surface treatment of Ti-6Al-4V for bio implant application, Lasers in Eng. 17, pp. 59-73.

[44] Edson, A. F., Alexandre, F. F., Rafael, A. B. and Antonio, C. G. (2011), Bioactive coating on titanium implants modified by Nd:YVO_4 laser, Appl. Surf. Sci. 257, pp. 4575-4580.

[45] Braga, F. J. C., Marques, R. F. C., Filho, E. A. and Guastaldi, A. C. (2007), Surface modification of Ti dental implants by Nd:YVO_4 laser irradiation, Appl. Surf. Sci. 253, pp. 9203–9208.

[46] Bini, R. A., Santos, M. L., Filho, E. A., Marques, R. F. C. and Guastaldi, A. C. (2009), Apatite layerings onto titanium surfaces submitted to laser ablation with different energy densities, Surf. Coat. Technol. 204, pp. 399–403.

[47] Borgioli, F., Galvanetto, E., Iozzelli, F. and Pradelli, G. (2005), Improvement of wear resistance of Ti-6Al-4V alloy by means of thermal oxidation, Mater. Lett. 59, pp. 2159-2162.

[48] Zivic, F., Babic, M., Mitrovic, S. and Todorovic, P. (2011), Interpretation of the friction coefficient during reciprocating sliding of Ti6Al4V alloy against Al2O3, Tribology in Industry 33(1), pp. 36-42.

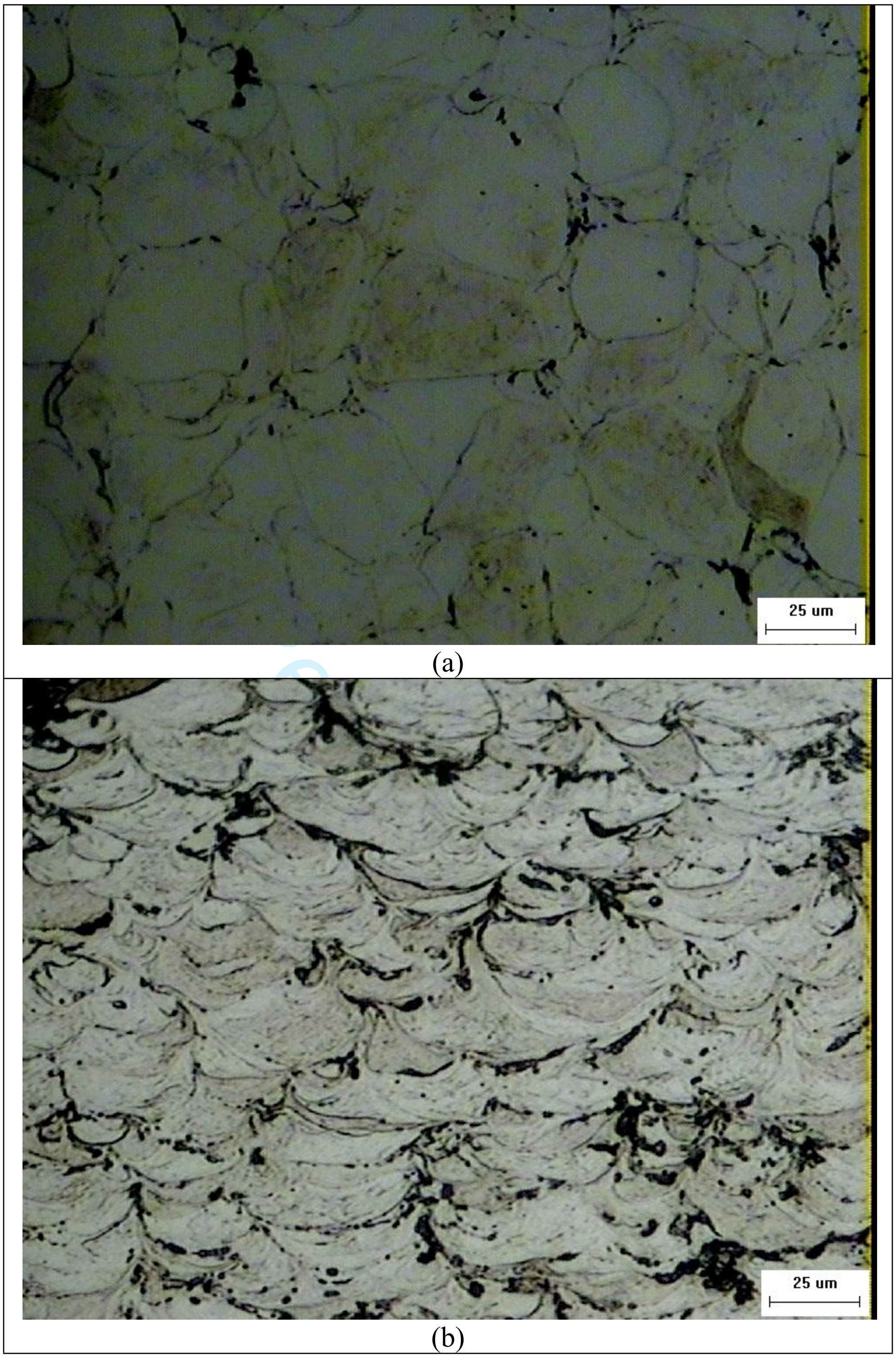

Fig. 1: (a) Surface and (b) cross-sectional microstructures of cold sprayed Ti64 coating observed after etching.

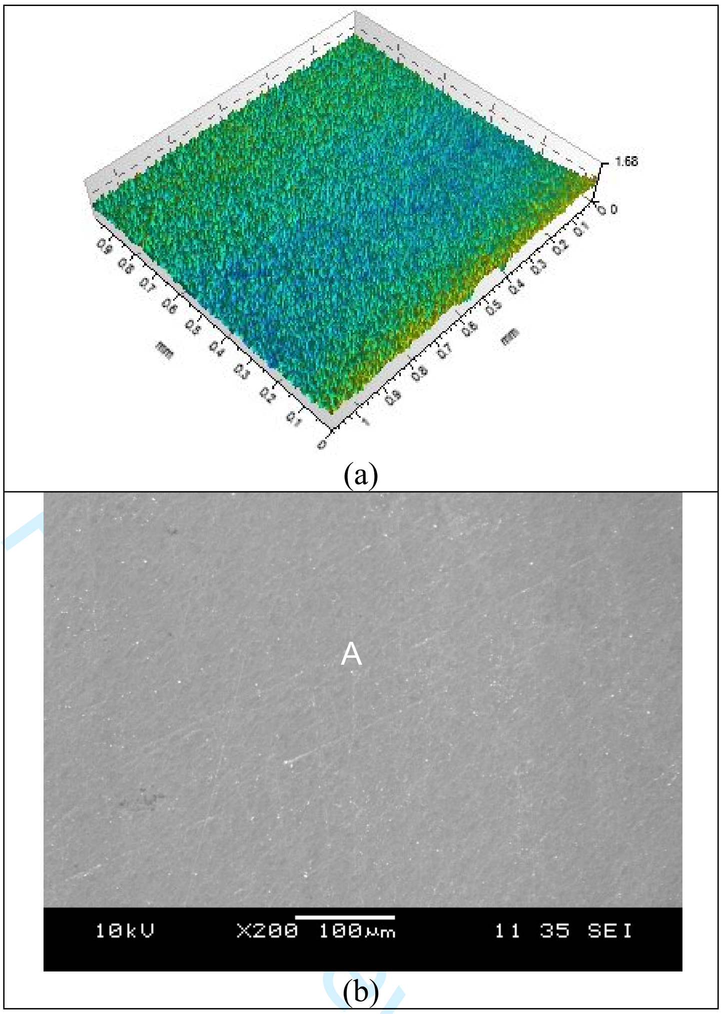

Fig. 2: Surface (a) topogrpahy and (b) morphology of untreated Ti64 coating.

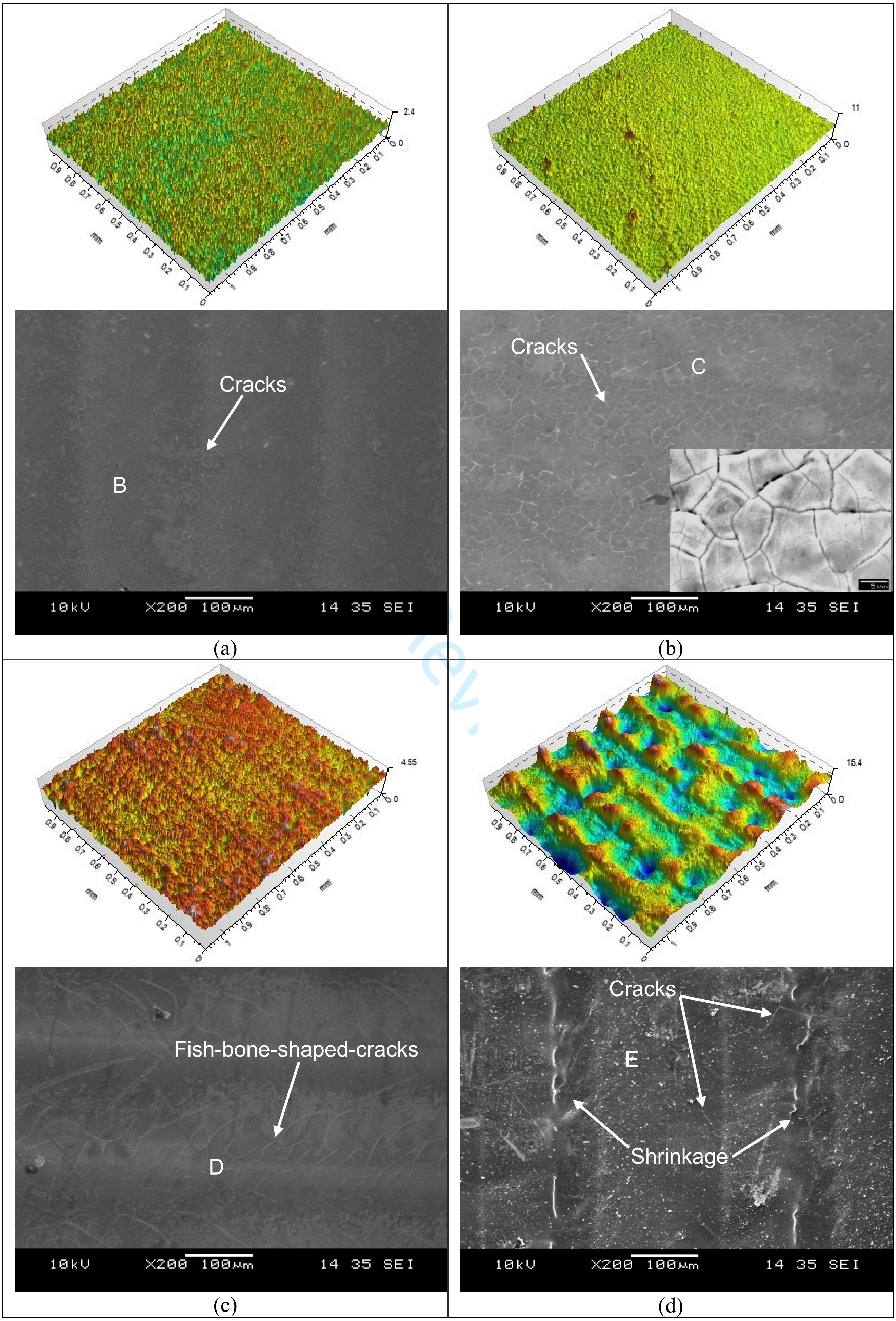
2.4
0.0
mm
11
0.0
mm
Cracks
B
10kV X200 100µm 14 35 SEI
Cracks
C
10kV X200 100µm 14 35 SEI
(a)
(b)
4.55
0
mm
15.4
0
mm
Fish-bone-shaped-cracks
D
10kV X200 100µm 14 35 SEI
Cracks
E
Shrinkage
10kV X200 100µm 14 35 SEI
(c)
(d)

Fig. 3: Surface topogrpahies (above) and morphologies (below) of laser treated Ti64 coatings with laser powers of (a) 50, (b) 100, (c) 150, and (d) 200 W. The inset in (b) shows magnified surface morphology of the same coating.

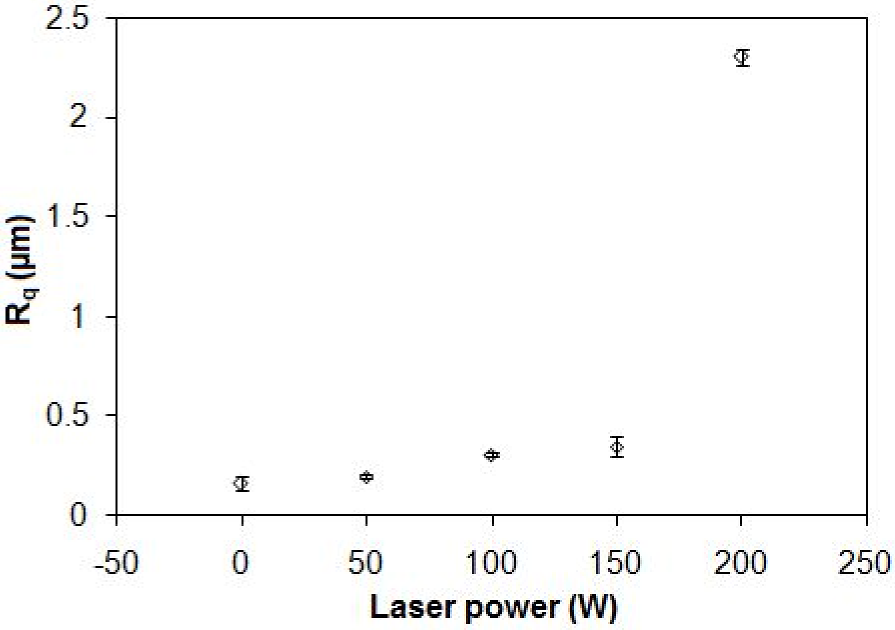

Fig. 4: R_q values of untreated Ti64 coating and laser treated Ti64 coatings with different laser powers. The laser power of "0" represents the untreated Ti64 coating.

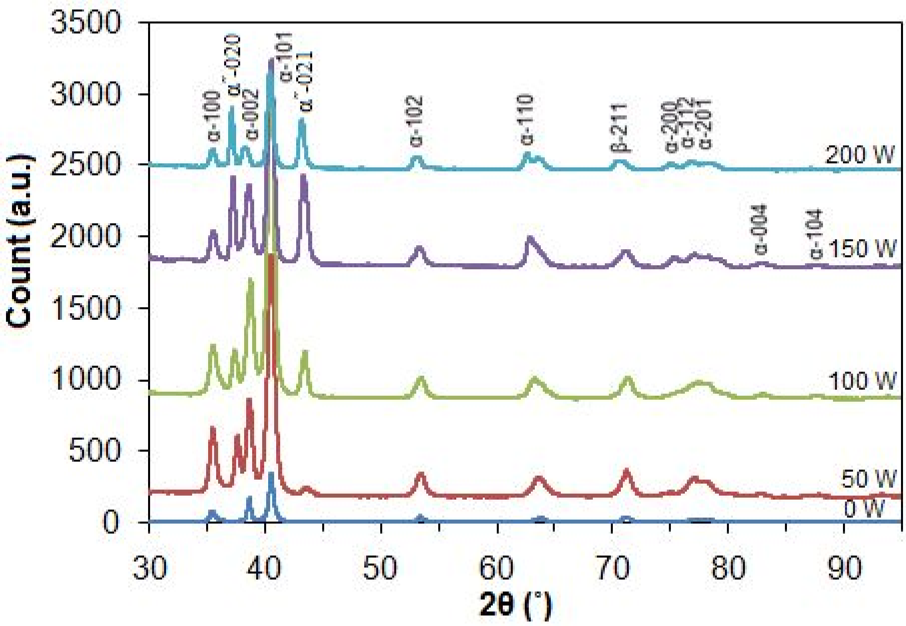

Fig. 5: XRD patterns of untreated Ti64 coating and laser treated Ti64 coatings with different laser powers. α″

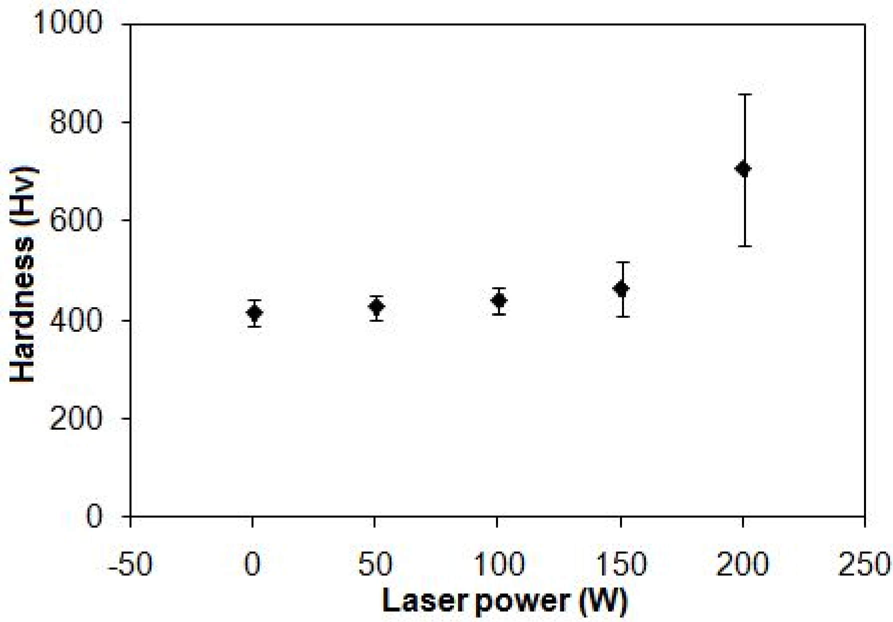

Fig. 6: Hardnesses of untreated Ti64 coating and laser treated Ti64 coatings with different laser powers.

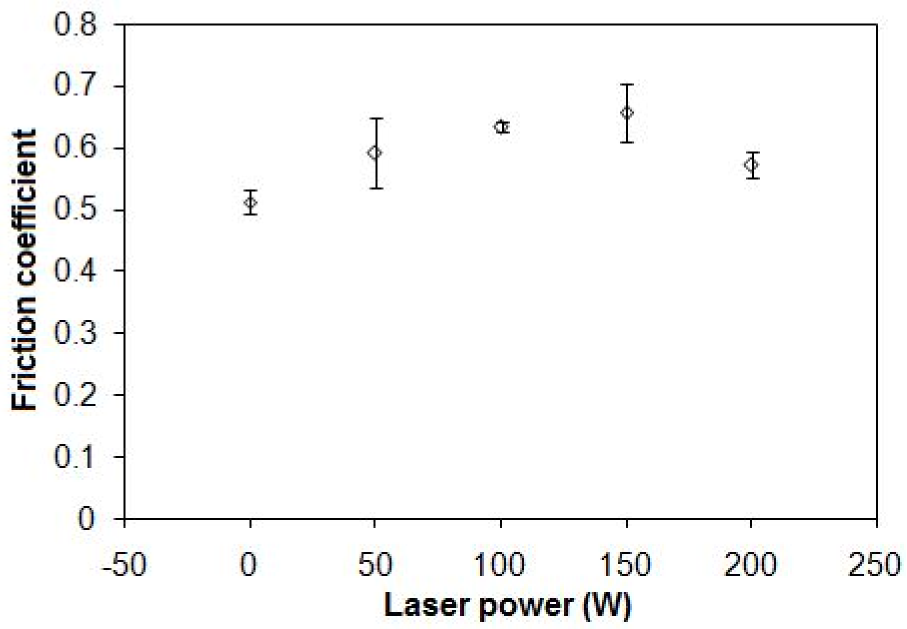

Fig. 7: Friction coefficients of untreated Ti64 coating and laser treated Ti64 coatings with different laser powers tested against 100Cr6 steel balls of 6 mm in diameter in a circular path of 1 mm in radius for 30000 laps at a sliding speed of 3 cm/s under a normal load of 1 N at RT.

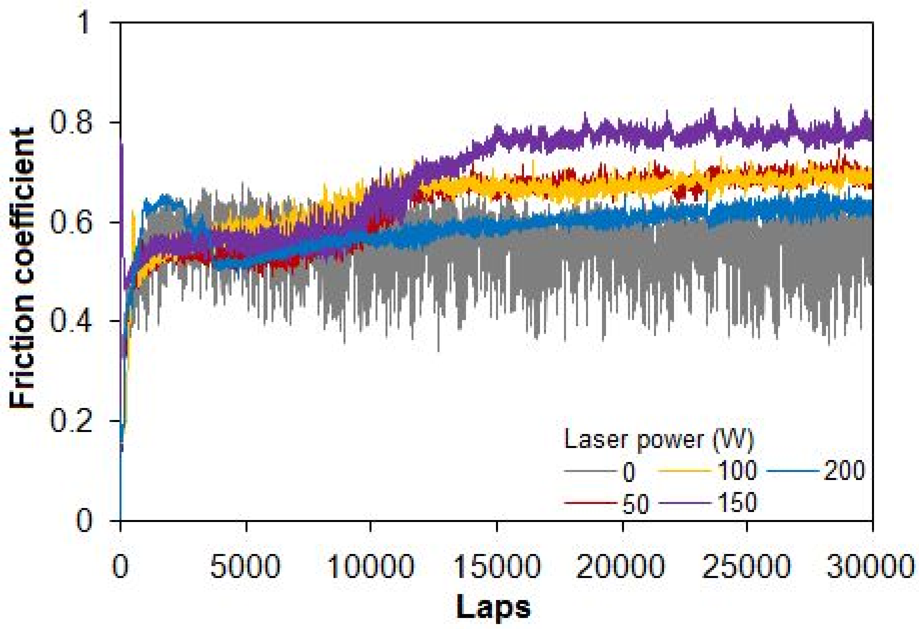

Fig. 8: Friction coefficients of untreated Ti64 coating and laser treated Ti64 coatings with different laser powers, tested under the same conditions as described in Fig. 7, as a function of the number of laps.

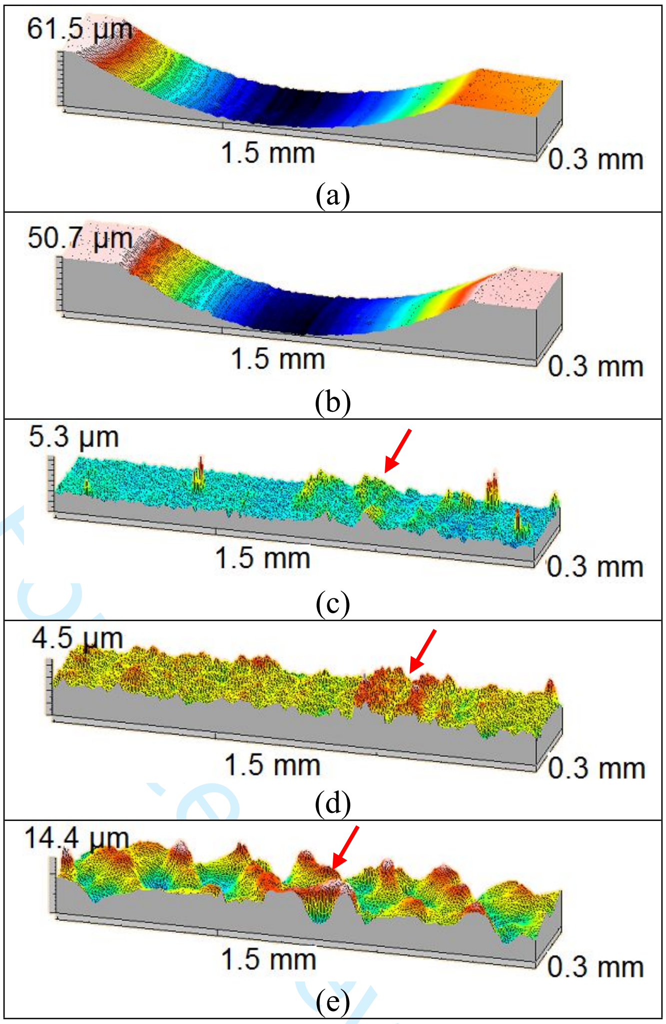

Fig. 9: Wear topographies of (a) untreated Ti64 coating and (b, c, d, and e) laser treated Ti64 coatings with laser powers of (b) 50, (c) 100, (d) 150, and (e) 200 W tested under the same conditions as described in Fig. 7. Red arrows indicate wear tracks of the laser treated Ti64 coatings.

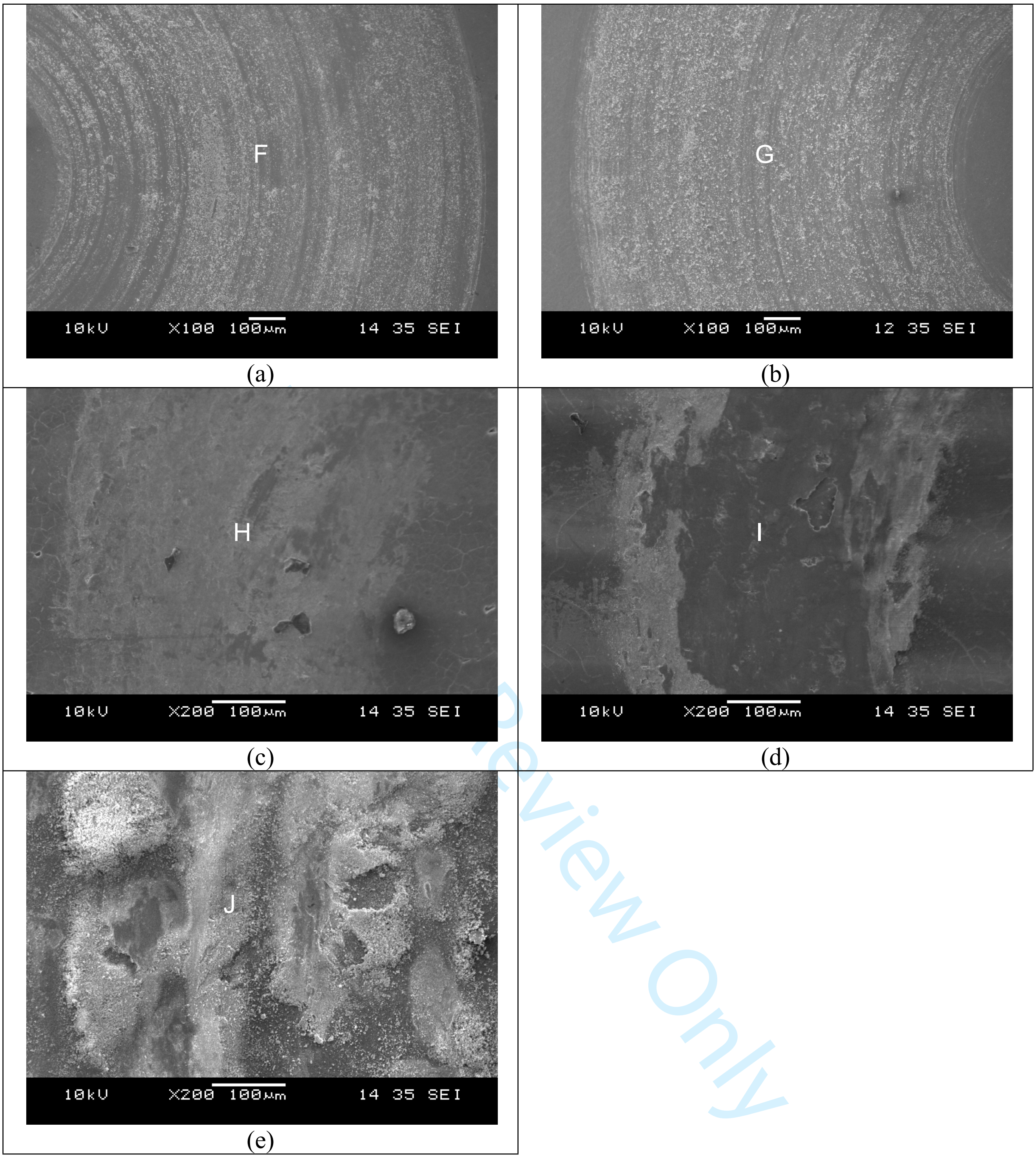

Fig. 10: Wear morphologies of (a) untreated Ti64 coating and (b, c, d, and e) laser treated Ti64 coatings with laser powers of (b) 50, (c) 100, (d) 150, and (e) 200 W tested under the same conditions as described in Fig. 7.

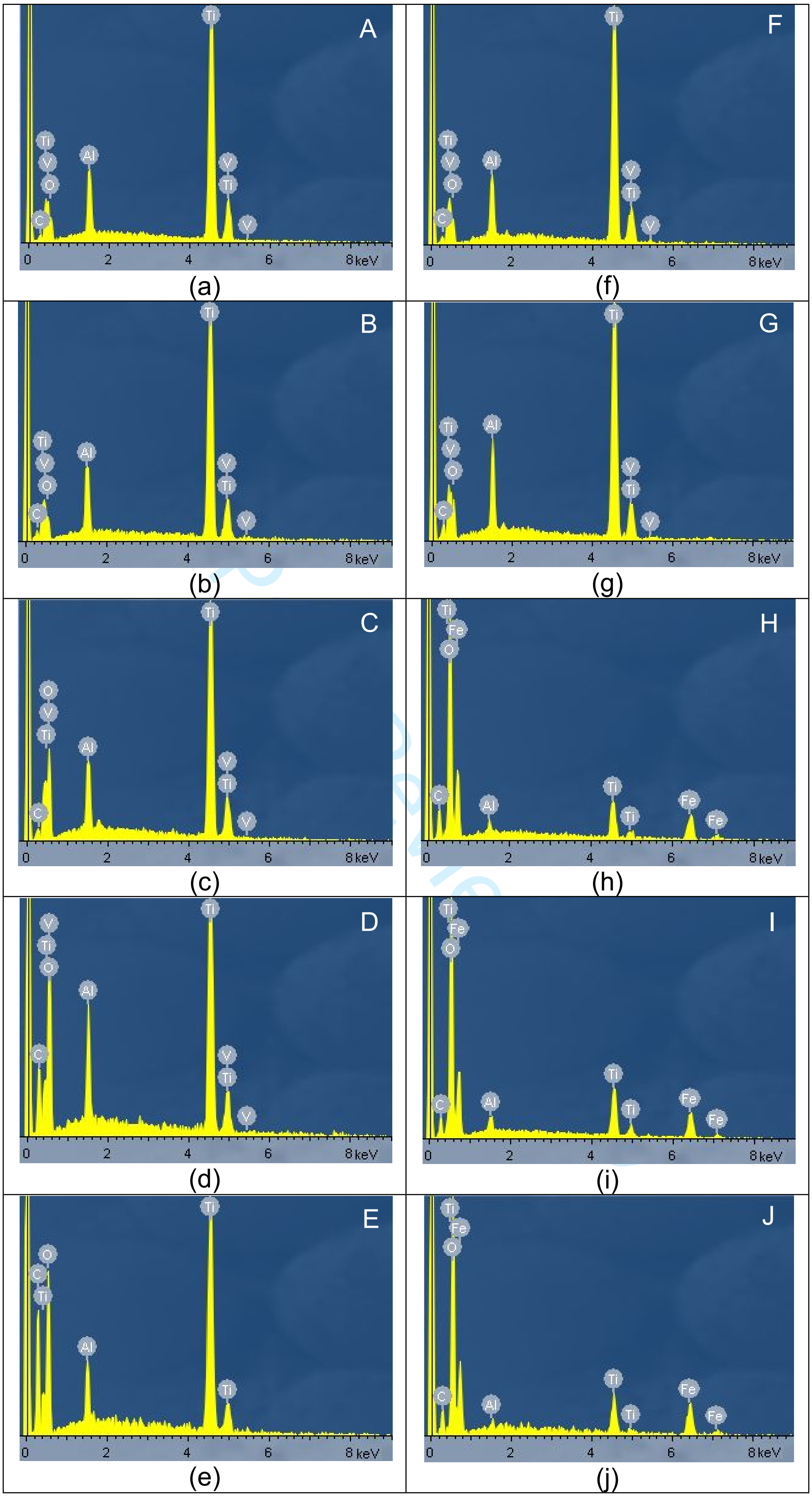
A
Ti
Ti V O C
Al
V Ti
V
0 2 4 6 8 keV
(a)
F
Ti
Ti V O C
Al
V Ti
V
0 2 4 6 8 keV
(f)
B
Ti
Ti V O C
Al
V Ti
V
0 2 4 6 8 keV
(b)
G
Ti
Ti V O C
Al
V Ti
V
0 2 4 6 8 keV
(g)
C
Ti
O V Ti C
Al
V Ti
V
0 2 4 6 8 keV
(c)
H
Ti Fe O
C
Al
Ti
Ti
Fe
Fe
0 2 4 6 8 keV
(h)
D
Ti
V Ti O
C
Al
V Ti
V
0 2 4 6 8 keV
(d)
I
Ti Fe O
C
Al
Ti
Ti
Fe
Fe
0 2 4 6 8 keV
(i)
E
Ti
O C Ti
Al
Ti
0 2 4 6 8 keV
(e)
J
Ti Fe O
C
Al
Ti
Ti
Fe
Fe
0 2 4 6 8 keV
(j)

Fig. 11: EDX spectra of (a and f) untreated Ti64 coating and (b, c, d, e, g, h, i and j) laser treated Ti64 coatings with laser powers of (b and g) 50, (c and h) 100, (d and i) 150, and (e and j) 200 W measured on their untested areas at location A in Fig. 2b, B in Fig. 3a, C in Fig. 3b, D in Fig. 3c, and E in Fig. 3d and on their wear tracks at location F in Fig. 10a, G in Fig. 10b, H in Fig. 10c, I in Fig. 10d, and J in Fig. 10e.

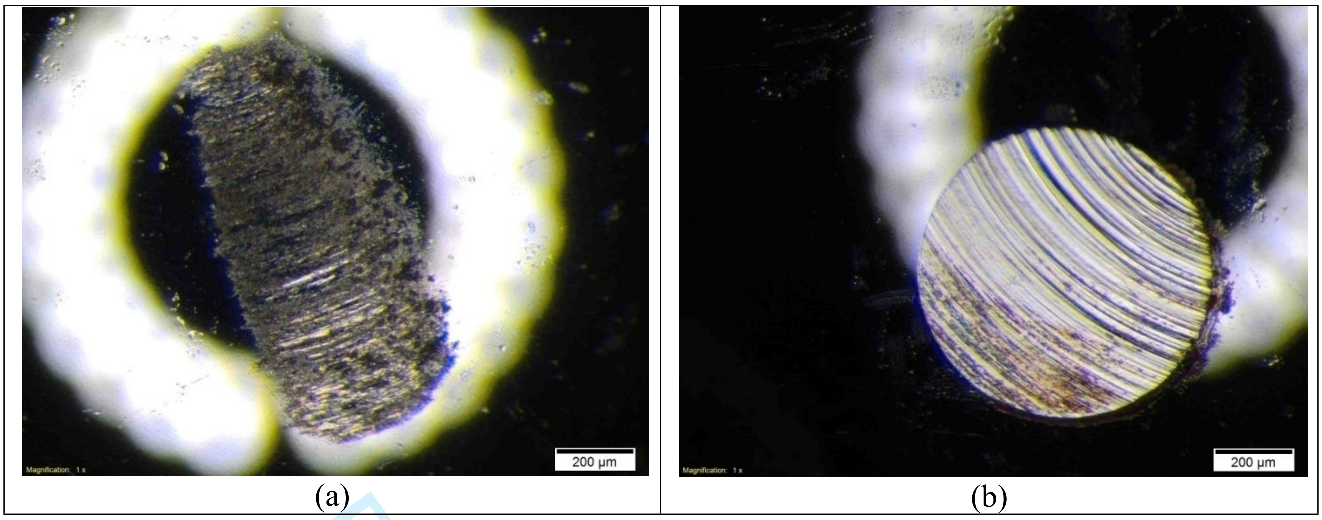

Fig. 12: Wear morphologies of 100Cr6 steel balls rubbed on (a) untreated Ti64 coating and (b) laser treated Ti64 coating with a laser power of 200 W under the same conditions as described in Fig. 7.

Response to comments of Editor and Reviewers

Effects of Nd:YAG laser surface treatment on tribological properties of cold sprayed Ti-6Al-4V coatings tested against 100Cr6 steel under dry condition

N. W. Khun, A. W. Y. Tan, W. Sun, E. Liu

First of all, authors would like to thank Editor and Reviewers for their critical comments on the manuscript (UTRB-3344). Amendments have been made to the revised manuscript as follows:

Response to Editor's comments

Comment 1: In experimental, what is the initial mean or maximum Hertzian contact stress/pressure? This is more important than just reporting the normal load/force and ball diameter.
Reply: Additional information was added in page 5 as highlighted with yellow background.

Comment 2: In experimental, why was 100Cr6 steel ball chosen as the counterface? Justification is needed.
Reply: The reason is that the hardness and wear resistance of the 100Cr6 steel balls are high enough to generate the significant wear of the cold sprayed Ti64 coatings. In addition, we would like to systematically compare the tribological results in this paper to our previous tribological results published in Ref. [5-8] in series.

Comment 3: in experimental, 30000 laps = what total sliding distance? This number should also be reported.
Reply: Additional information was added in page 5 as highlighted with yellow background.

Comment 4: Fig. 5: some of the diffraction peaks in the 35 to 45 2 theta range are not indexed to a particular phase(s)? They should be added.
Reply: The two peaks at about 37.5 and 43.5 degree were identified in Fig. 5. Additional information with an additional reference was added in page 7 as highlighted with yellow background.

Comment 5: Fig. 6 caption, hardness is misspelled.
Reply: It was corrected in page 25 as highlighted with yellow background.

Comment 6: Related to point 2 above, there is Fe oxidation in the wear track due to adhesive wear of the steel counterface. This could be biasing the friction and wear results, i.e., the true friction and wear behavior of Ti64 is not being measured due to counterface wear. This should be addressed on the bottom of 10.
Reply: In this manuscript, we systematically presented the effects of Nd:YAG laser surface treatment on the friction and wear results of the cold sprayed Ti64 coatings tested against 100Cr6 steel balls under dry condition. It is sure that changing the counter balls,

such as their shapes, sizes and materials, will apparently change the coefficient of friction and wear rate of the coatings. e.g. If we use ceramic balls which have much higher wear resistance than steel balls, the ceramic balls would generate the much higher wear of the coatings without significant wear of the balls (However, we believe that the high wear resistance of the laser treated Ti64 coating with 200 W can generate the apparent surface wear of its counter ceramic ball). The cofficient of friciton and wear rate of the coatings tested against the ceramic balls will be differrent from those of the same ones tested against the steel balls. It is difficult to measure the true friction and wear of the coatings without the effects of counter ball wear, especially during prolonged sliding test for the reliable measurement. It is the tribological behavior of two solid surfaces in cotact subject to relative motion. However, we modified the whole manuscript in order to clearly point out the tribological properties of the laster treated Ti64 coatings tested against 100Cr6 steel balls under dry condition as highlighted with yellow background.

Response to Reviewer 1's comments

Comment 1: The author claims that the Ti6Al4V coatings were deposited using He as a propellant gas at 2.5 MPa and 950 oC. It is known from the literature that He accelerates particles to velocities > 1000 m/s (when sprayed at 4 MPa and 350 oC) which results in dense Ti6Al4V deposits (porosity < 2%). Here, the gas temperature was significantly higher but based on the optical images shown (Fig. 1b) it can be observed that there was a significant amount of porosity in the coatings. The author should measure the porosity in the coatings and explain the reasons for porosity despite using He as propellant gas. Also, the author should check if the reported spray parameters and propellant gas were correct.
Reply: The cold spray process parameters used in this study are correct. Although we use the same cold spray process parameters to produce Ti64 coatings, the resulted microstructures and porosity levels can be significantly different depending on applied cold spray systems (PCS100 and 5/11 cold spray systems) and their nozzle designs. In this study, the gas temperature used was significantly higher as mentioned above, but the gas pressure was lower so that our coating microstructures could not be compared with others in the literature. However, apparent flatteness of cold sprayed particles can be found in the optical micrograph due to their severe deformation which is responsible for the compacted microstructure of the coating. Additional information was provided in page 5 as highlighted with yellow background.

Comment 2: Was there a wear scar on the counterface that slid on all the Ti6Al4V coatings (as-deposited and laser treated (50, 100 and 150 W)? If yes, the author should present the optical or SEM images of the worn counterfaces and calculate the respective wear volumes.
Reply: There were wear scars on all the counterfaces that slid on the untreated and laser treated Ti6Al4V coatings. However, we are not able to provide their respective wear volumes at this stage. We did not provide additional images of the worn counterfaces to avoid the inflation of the manuscript with too many images. Fig. 12 is sufficient to understand the wear behavior of the counterfaces. The results are good enough to understand the effects of Nd:YAG laser surface treatment on the tribological properties of

cold sprayed Ti64 coatings tested against 100Cr6 steel balls. However, we added some information in page 11 as highlighted with yellow background.

Comment 3: The author has combined the results and discussion sections. Sometimes it is difficult to follow if the observations made are based on the results obtained in the present work or from the literature. The author should separate these sections for a better flow of the results.
Reply: We would like to maintain our current manuscript style to discuss the results based on figures.

Comment 4: The author repeats many observations made in the results and discussion section in the conclusions. The author should highlight only the major conclusions of the work in the conclusion section.
Reply: The conclusions were revised.

Response to Reviewer 2's comments

Comment 1: The roughness values of samples after laser treatment are not the same. Firstly, it will strongly affect tribological performance. Secondly, the application of samples with high roughness and cracks are also strongly limited. Therefore, it is strongly suggested to compare samples with same roughness.
Reply: We are not able to provide the tribological properties of the laser treated Ti64 coatings with the same surface roughness because we do not know the thicknesses of laser treated surface layers for different laser powers and are not able to control the removal of the laser treated surface layers by polishing. In addition, we would like to get a fundamental understanding of the effects of laser induced surface patterns on the tribological properties of the laser treated Ti64 coatings. We believe that we have systematically investigated the effects of Nd:YAG laser surface treatment on the tribological properties of the cold sprayed Ti64 coatings tested against 100Cr6 steel balls.

Comment 2: Why the authors chose 100Cr6 as wear mate? Typically, tribological performance strongly depends on wear mate. For example, in Figs.9, the laser-treated Ti64 coatings with laser powers of 100-200W do not show measurable wear tracks on their surfaces. It might be just due to laser treated surface having higher hardness than 100Cr6 steel. In Fig.11 (h)/(i)/(j) (100W-200W), there's clear Fe peak. It means there's residual Fe debris from steel ball. But there is not Fe peak for 0W and 50W, it might be due to test samples (0W and 50W) having lower hardness than 100 Cr6 steel, therefore, the authors could see clear wear tracks on test samples.
Reply: The reason is that the hardness and wear resistance of the 100Cr6 steel balls are high enough to generate the significant wear of the cold sprayed Ti64 coatings. In addition, we would like to systematically compare the tribological results in this paper to our previous tribological results published in Ref. [5-8] in series. Please refere to the reply to Editor's comment 6.

Comment 3: What are the effective depths of laser-treatment? Any difference under different laser powers? For multi-layers samples, the hardness strongly depends on applied load and thickness of each layer in addition to hardness of each layer. Therefore, the increase of hardness with increasing laser power shown in Fig.7 might be also contributed by increase of effective depth of laser treatment. The increase of laser power might increase both effective depth and hardness value of laser treated layer. It is interesting and necessary to differentiate these two impacts in this study. Since these results could explain the data shown in Figs9-11 more clearly.
Reply: It is possible that the increase of laser power could increase the effective depth of laser treatment and consequently the surface hardness of the laser treated Ti64 coatings. The micro-hardness of the laser treated Ti64 coatings measured under a normal load of 1.96 N is sufficient to understand the effects of surface hardness on their surface wear resistance measured under a normal load of 1 N. In this study, we only have the micro-hardness data of the laser treated Ti64 coatings so the hardness data is focused to explain the improved surface wear resistance of the coatings. However, a hypothesis based on reviwer's suggestion was added in page 7 as highlighted with yellow background.

Comment 4: For ball-on-disk test, the steel ball diameter is ~ 6mm, but the radius of circular path is only 1mm, which might be too small since the contact radius might be close to 1mm, as shown in Figs.12.
Reply: The 1 mm radius of circular path used was not small for the micro-tribological test, which was also used in our previous works published in Ref. [5-8].

Comment 5: Fig.2 showed surface topography and morphology of untreated Ti64 coating. It might be better to include surface topography and morphology of laser-treated Ti64 coating as comparison.
Reply: The surface topographies and morphologies of the laser treated Ti64 coatings with laser powers of 50-200 W were already shown in Fig. 3.

Comment 6: Rq value typically depends on scan size, what's the scan size used to measure Rq in Fig.4?
Reply: A scan size of 1 mm × 1 mm was added in page 5 as highlighted with yellow background.

Comment 7: In Fig.5, the authors did not label two peaks @ ~ 37.5 degree and ~ 44 degree, what are the meanings of these two peaks?
Reply: Two peaks at about 37.5 and 43.5 degree were labelled in Fig. 5. Additional information with an additional reference was added in page 7 as highlighted with yellow background.

Comment 8: In Fig.7, it might be better to convert unit of hardness to SI unit.
Reply: We would like to maintain the "Hv" unit of hardness in Fig. 6 in order to compare with our previous results published in Ref. [5-8]. However, the converted hardness values in SI units were added in page 7 as highlighted with yellow background.